

ORIGINAL ARTICLE

Isolated Focal Dystonia as a Disorder of Large-Scale Functional Networks

Giovanni Battistella¹, Pichet Termsarasab^{1,†}, Ritesh A. Ramdhani^{1,†},
Stefan Fuertinger¹ and Kristina Simonyan^{1,2}

¹Department of Neurology and ²Department of Otolaryngology, Icahn School of Medicine at Mount Sinai, New York, NY, USA

Address correspondence to Kristina Simonyan, Department of Neurology, Icahn School of Medicine at Mount Sinai, One Gustave L. Levy Place, Box 1137, New York, NY 10029, USA. Email: kristina.simonyan@mssm.edu

[†]These authors contributed equally to this manuscript.

Abstract

Isolated focal dystonias are a group of disorders with diverse symptomatology but unknown pathophysiology. Although recent neuroimaging studies demonstrated regional changes in brain connectivity, it remains unclear whether focal dystonia may be considered a disorder of abnormal networks. We examined topology as well as the global and local features of large-scale functional brain networks across different forms of isolated focal dystonia, including patients with task-specific (TSD) and nontask-specific (NTSD) dystonias. Compared with healthy participants, all patients showed altered network architecture characterized by abnormal expansion or shrinkage of neural communities, such as breakdown of basal ganglia–cerebellar community, loss of a pivotal region of information transfer (hub) in the premotor cortex, and pronounced connectivity reduction within the sensorimotor and frontoparietal regions. TSD were further characterized by significant connectivity changes in the primary sensorimotor and inferior parietal cortices and abnormal hub formation in insula and superior temporal cortex, whereas NTSD exhibited abnormal strength and number of regional connections. We suggest that isolated focal dystonias likely represent a disorder of large-scale functional networks, where abnormal regional interactions contribute to network-wide functional alterations and may underline the pathophysiology of isolated focal dystonia. Distinct symptomatology in TSD and NTSD may be linked to disorder-specific network aberrations.

Key words: community structure, dystonia, graph theory, independent component analysis, resting-state fMRI

Introduction

Dystonia is a rare, debilitating neurological disorder characterized by abnormal movements and postures, which usually cause emotional stress and social embarrassment of the affected individuals. While the symptomatology of dystonia is well defined, its pathophysiology continues to remain unclear. Common to all forms of dystonia, involuntary co-contractions of agonist and antagonist muscles that produce abnormal movements are seemingly related to motor entrainment, triggering a concatenation of several physiological aberrations, such as loss of surround inhibition, maladaptive neuroplasticity, and abnormal

sensorimotor processing and integration (Quartarone and Hallett 2013). Neuroimaging studies have started shedding light on neural functional and structural correlates underlying these alterations, hinting that dystonia may represent a network disorder. Starting with Eidelberg and colleagues, who described generalized dystonia as an abnormal metabolic network disorder through a series of positron emission tomography studies back in the 1990s (Eidelberg et al. 1995, 1998; Carbon et al. 2004; Asanuma et al. 2005; Carbon and Eidelberg 2009; Niethammer et al. 2011), recent MRI studies mapped selected components of neural networks in patients with focal dystonia, with the cumulative

evidence suggesting that isolated focal dystonias, too, may represent a network disorder (Neychev et al. 2011; Zoons et al. 2011; Lehericy et al. 2013; Quartarone and Hallett 2013; Ramdhani and Simonyan 2013). Among these, resting-state studies examining regional functional connectivity in patients with writer's cramp have found decreased connectivity in the left primary somatosensory region with concomitant increases in the left putamen (Mohammadi et al. 2012) as well as functional decoupling of the left dorsal premotor cortex and left superior parietal lobe (Delnooz et al. 2012). Similarly, the sensorimotor network was found to be altered in patients with cervical dystonia, with abnormalities extending to the primary visual and executive control networks (Delnooz et al. 2013), whereas resting-state network changes in blepharospasm were related to the default mode network, including the thalamus and cortico-striato-pallidal regions (Yang et al. 2013). Another study examining structural brain organization has reported the presence of common and distinct abnormalities across different forms of dystonia (Ramdhani et al. 2014), suggesting that structural changes may underlie alterations of neural activity and contribute to the formation of functionally abnormal brain networks in this disorder. Taken together, the results of these studies indicate that, while the pathophysiology of dystonia may be rooted around the same factors, different subclasses of dystonia may follow divergent pathophysiological mechanisms. However, despite the recent progress in mapping regional neural correlates of dystonia pathophysiology, direct demonstration of whether isolated focal dystonia indeed represents a large-scale network disorder due to concurrent or subsequent dysfunction and abnormal communication between different regions within the network (Neychev et al. 2011; Lehericy et al. 2013) still remains scant. Further, it is unclear whether such large-scale neural re-organization is present across different forms of focal dystonia or is rather a specific feature of a particular form of dystonia.

To provide experimental evidence for the envisioned concept of isolated focal dystonia as a network disorder, we examined the large-scale topology of functional brain networks across different forms of dystonia by using a two-tiered approach of network analyses, including graph theoretical (Bullmore and Sporns 2009) and multivariate independent component analyses (ICA) (Beckmann and Smith 2004) of resting-state functional MRI (fMRI) data. It has been shown that resting-state networks, which are based on the measure of intrinsic low frequency physiological fluctuations in the blood oxygen level-dependent (BOLD) signal, reflect the organization of both structural and task-related functional brain networks (Biswal et al. 1995; Damoiseaux and Greicius 2009; Smith et al. 2009). The

choice of resting-state fMRI in this study was made to circumvent the challenge associated with the implementation of the task-related fMRI design across different forms of dystonia, which exhibit distinct symptoms, thus making the choice of a single, commonly affected task production unfeasible. Furthermore, because the explanation of functional changes across different forms of dystonia may sometimes be ambiguous due to a combination of motor and sensory components (Ramdhani and Simonyan 2013), examination of the resting-state functional networks was expected to provide a more uniform and coherent understanding of network alterations. As different aspects of neural network architecture can be assessed using complementary analytical approaches, we employed ICA to investigate functional connectivity among specific resting-state networks across different forms of dystonia and graph theoretical analysis to examine the global and local features of functional network architecture in the same patients.

We hypothesized that functional brain networks in isolated focal dystonia undergo widespread re-organization not limited to the basal ganglia and/or cerebellar circuitry as historically envisioned (Burton et al. 1984; Marsden 1984; Berardelli et al. 1985; Jinnah and Hess 2006). Furthermore, because our cohort included patients with both task-specific dystonia (TSD), such as writer's cramp and spasmodic dysphonia, and nontask-specific dystonia (NTSD), such as cervical dystonia and blepharospasm, we hypothesized that the clinical phenomenon of task specificity in dystonia would have an additional impact on network abnormalities, that is, TSD patients would exhibit greater alterations of sensorimotor and executive networks necessary for the proper control of skilled and highly learned tasks, such as writing and speaking.

Methods

Participants

We recruited 15 TSD patients (8 with spasmodic dysphonia and 7 with writer's cramp), 18 NTSD patients (9 with cervical dystonia and 9 with blepharospasm), and 15 healthy participants (see detailed demographics in Table 1). The grouping of patients was based on dystonias affecting highly learned and uniquely human behaviors, such as speaking and writing, vs. dystonias affecting more stereotyped behaviors, such as blinking and positioning of the neck, as described earlier (Ramdhani et al. 2014). Although dystonias affecting different body parts may have alterations in different brain regions (e.g., hand area vs. larynx area of the primary motor cortex), this grouping choice was

Table 1 Demographics of participants

Type of dystonia	Task-specific dystonia (n = 15)		Nontask-specific dystonia (n = 18)		Healthy participants (n = 15)	P value
	Spasmodic dysphonia	Writer's cramp	Cervical dystonia	Blepharospasm		
Number of participants	8	7	9	9	15	N/A
Age (years; mean ± standard deviation)	59.9 ± 11.4	53.3 ± 9.4	55.2 ± 12.8	60.1 ± 8.1	49.7 ± 13.0	≥0.08
Gender (Female/Male)	6 F/2 M	3 F/4 M	7 F/2 M	9 F	8 F/7 M	≥0.23
Dystonia duration (years; mean ± standard deviation)	13.2 ± 10.2		9.6 ± 7.5		N/A	0.27
Symptom severity (BFMDRS; mean ± standard deviation)	3.0 ± 0.9		3.3 ± 2.5		N/A	0.70
Handedness (Edinburgh Inventory)	All: Right					
Genetic status	All: Negative for DYT1, DYT6, DYT4, and DYT25					

Note: BFMDRS, Burke–Fahn–Marsden Dystonia Rating Scale; N/A, not applicable.

specifically made to examine the characteristic features of the large-scale networks that may underlie the phenomenon of task specificity in dystonia.

All participants were right-handed, and none had any past or present history of psychiatric or neurological problems (except for the restrictive forms of isolated focal dystonia in the patient groups). All patients were fully symptomatic at the time of study participation; those who received botulinum toxin injections participated in the study at least 3 months after the last treatment. Neuroradiological evaluation found normal brain structure in all subjects without any gross abnormalities. The duration of the disorder was 13.2 ± 10.2 years in the TSD group and 9.6 ± 7.5 years in the NTSD group. The severity of dystonia was 3.0 ± 0.9 in TSD patients and 3.3 ± 2.5 in NTSD patients as assessed using the Burke-Fahn-Marsden Dystonia Rating Scale, which comprises a movement scale on dystonia provoking and severity factors (scored 0–4 based on the neurological examination) and a disability scale (scored 0–4 based on the patient's opinion of his/her disability in daily activities) (Burke et al. 1985). These groups did not differ significantly in their age, gender, duration, or severity of the disorder (all $t \leq 1.9$, $P \geq 0.08$, Table 1), and the duration of disorder was not associated with its severity (all $r \leq 0.39$, $P \geq 0.23$). None of the participants were carriers of TOR1A (DYT1), THAP1 (DYT6), TUBB4A (DYT4), or GNAL (DYT25) mutations as confirmed by genetic screening.

All participants provided written informed consent, which was approved by the Institutional Review Board of the Icahn School of Medicine at Mount Sinai.

MRI Acquisition Protocol

All patients and healthy participants were scanned on a 3T scanner equipped with an 8-channel head coil. Resting-state fMRI data were acquired using a single-shot echo planar imaging (EPI) gradient-echo sequence with repetition time (TR) 2000 ms, echo time (TE) 30 ms, flip angle 90° , field of view (FOV) 240 mm, pixel size 3.75×3.75 mm, and 33 slices of 4 mm covering the whole brain. The scan lasted 5 min, corresponding to the acquisition of 150 volumes. The light in the scanner room was minimized, and all participants were instructed to lie with their eyes closed, to think of nothing in particular, and not to fall asleep. The scanning protocol included a T_1 -weighted gradient-echo sequence (MPRAGE) with 172 contiguous slices, 1 mm isotropic voxel, TR 7.5 ms, TE 3.4 ms, flip angle 8° , inversion time displacement 819 ms, and FOV 210 mm for anatomical reference of the functional images. During the scanning session, restricted padding of the participant's head in the coil minimized head movements; all participants were monitored during the entire scanning session for excessive movements as well as for their alertness.

Data Analysis

Image processing was performed using a combination of FSL, SPM8, and AFNI software packages. All images were visually inspected for motion artifacts before processing. To assess head motion in the healthy participant, TSD and NTSD groups, we calculated the root mean square of the 6 motion parameters, including 3 translations and 3 rotations, along the XYZ axes in each group. Mean \pm standard deviation root mean square motion values were as follows: healthy participants (0.14 ± 0.05), TSD (0.24 ± 0.3), and NTSD (0.22 ± 0.11). A one-way analysis of variance (ANOVA) found no significant differences in root mean square motion across the groups ($F_{2,45} = 1.14$, $P = 0.33$). Therefore, none

of participants were excluded from the study due to motion artifacts. None of participants experienced dystonic symptoms during the scan acquisition.

Following the removal of the first 4 volumes of the resting-state acquisition to avoid possible T_1 stabilization effects, each brain volume was corrected for residual motion, masked to remove nonbrain voxels, and high-pass filtered using a cutoff frequency of 0.01 Hz (Gaussian-weighted least squares straight line fitting). To further control for the effects of possible movement and physiological noise, each 4D time series were regressed using eight parameters, including 2 parameters for the white matter and cerebrospinal fluid mean signals and 6 motion parameters, which were calculated during image realignment. The white matter and cerebrospinal fluid covariates were extracted through automatic segmentation of the anatomical image in each subject's native space into gray matter, white matter, and cerebrospinal fluid using the unified segmentation approach (Ashburner and Friston 2005) implemented in SPM8. The white matter and cerebrospinal fluid maps were thresholded at 90% of tissue probability and then applied to each time series in each individual. All voxels in these masks were then averaged across all time series to extract nuisance regressors. The functional images were co-registered to the respective anatomical acquisition using a 6-parameter rigid transformation, normalized to the standard Talairach–Tournoux space using affine registration and further optimized using a nonlinear normalization algorithm. The obtained images were smoothed with a Gaussian kernel full width at half maximum of 5 mm and mean-based intensity normalized.

Functional Connectivity: Graph Theoretical Analysis

Each participant's residual 4D time series were submitted to graph theoretical analysis to examine large-scale functional network topology. For this, functional nodes (i.e., regions) were defined using a nonoverlapping 212-region parcellation of the whole brain, consisting of 142 cortical, 36 subcortical, and 34 cerebellar regions, which were derived from the cytoarchitectonic maximum probability and macrolabel atlases (Eickhoff et al. 2005; Furtinger et al. 2014). Zero-lag Pearson's correlation coefficients were computed between all pairs of mean time series calculated across all voxels within each region in every participant. These pairwise correlations formed the functional edges of the graphs, resulting in whole-brain fully weighted undirected networks. Group-averaged networks were calculated for healthy participant, TSD and NTSD groups, respectively. Network completeness was assessed by calculating each graph's density given by the ratio of present to maximally possible connections. The analysis of graph metrics was conducted using the Brain Connectivity Toolbox (Rubinov and Sporns 2010) and an in-house developed code library (<http://research.mssm.edu/simonyanlab/analytical-tools/>).

To examine global features of network architecture, we assessed the topology of functional communities, or modules. To ensure validity of the community analysis, networks were thresholded to a density level of 50% by removing “weak” edges relative to the maximum weight within each network. A module was defined as a group of nodes that had many connections to other nodes within the module but few connections to nodes outside the module (Bullmore and Bassett 2011). The optimal modular decomposition was computed using a Louvain fast-unfolding algorithm (Blondel et al. 2008) followed by an iterative fine tuning (1000 iterations) of the module partition (Sun et al. 2009) to guarantee stability of the resulting partitions. Thus, in contrast to

classical clustering techniques, such as the K-means algorithm (Bishop 2006), the employed modular decomposition did not impose an a priori number of modules for the final partition of the network. The grouping of nodes into modules was based on the spectral features of the network and not on the spatial, anatomical proximity to the other brain regions, that is, regions exhibiting numerous pairwise correlations (i.e., functional connections) among each other comprised a functional community. The between-group similarity of modular decompositions was estimated by calculating the normalized mutual information (NMI) of the corresponding community affiliation vectors, with NMI = 0 showing the lowest similarity and NMI = 1 showing the highest similarity in the networks between the groups (Rubinov and Sporns 2010).

To assess characteristic features of regional functional connectivity, we further computed the nodal degree, which is expressed as the number of connections that link a node to the rest of the network, and the nodal strength, which reflects the sum of weights of links connected to the node (Rubinov and Sporns 2010) in each group. Statistical differences in these metrics between all patients and healthy participants as well as between TSD and NTSD groups were assessed directly using a two-sample t-test at $P \leq 0.05$, corrected for multiple comparisons. To examine the most influential nodes within a graph, we additionally assessed hub nodes defined as pivotal regions of information transfer, which facilitate integration between the different nodes of a functional network and assure network resilience (Rubinov and Sporns 2010). We considered a node to be a network hub if the nodal strength and degree were at least 1 standard deviation greater than the average strength/degree of the network (Bassett and Bullmore 2006; Shu et al. 2011).

Functional Connectivity: Independent Component Analysis

As a complimentary step, we used ICA to examine the connectivity patterns of specific networks between all patients and healthy participants and between TSD and NTSD patients. Pre-processed time series in all subjects were concatenated and decomposed into spatially independent components using a temporal concatenation approach (Beckmann and Smith 2004) implemented in the MELODIC (Multivariate Exploratory Linear Optimized Decomposition into Independent Components) tool of the FSL software package. All resultant components were visually examined, and the sensorimotor and frontoparietal components were extracted as relevant to dystonia pathophysiology for further analysis. To evaluate between-group differences in functional connectivity among the spatial components identified by the temporal concatenation ICA, we employed a dual regression analysis (Filippini et al. 2009; Leech et al. 2011). This algorithm permits identification of participant-specific temporal dynamics and associated temporal maps for each component of interest. For this, we used each participant's residual 4D time series after removing the 8 nuisance variables. Voxel-based inferential statistics in each component of interest were performed using a one-way ANOVA employing the individual Z-value maps of the dual regression at 3 levels (healthy participant, TSD, and NTSD groups). Statistical significance was set at $P \leq 0.05$ after family-wise error (FWE) correction for multiple comparisons over the component of interest.

Relationship Between Different Network Alterations and Their Clinical Correlates

To assess the direct relationships between different network alterations found using ICA and graph theoretical analysis, we

performed a conjunction analysis, which allowed us to examine the results of 2 independent analyses within the same statistical map, highlighting significantly different voxels that do and do not overlap across these complimentary analytic approaches. For this, we used the statistical maps of significant clusters (FWE-corrected $P \leq 0.05$) from the patients vs. healthy participants ICA contrast and significant hub regions from graph analysis to compute the conjunction maps. We then used Pearson's correlation coefficients to examine the relationship of the mean Z-score measures in these overlapping alterations with the duration and severity of dystonia symptoms as assessed with Burke-Fahn-Marsden Dystonia Rating Scale at $P \leq 0.05$.

Results

Graph Theoretical Analysis

At a large-scale level, we found abnormal network architecture in patients vs. healthy participants as well as in TSD vs. NTSD patients. In all participant groups, we identified 5 interrelated functional communities (Fig. 1). However, in the both patient groups, differences in nodal module assignment caused expansion or reduction of these communities, leading to a reconfiguration of the global network topology and the loss of normal hemispheric asymmetry in the community structure. Quantitatively, the partition distance between network communities showed higher similarity when comparing TSD and NTSD groups (NMI = 0.7) than in TSD/NTSD vs. healthy participant groups (NMI = 0.5 and 0.4, respectively), confirming the presence of topological abnormalities in large-scale networks in patients with isolated dystonia.

Specifically, in healthy participants, the largest functional community of 63 nodes (Module V) included the cerebellum, basal ganglia, and thalamus and was followed by Module IV (48 nodes) in the right sensorimotor, parietal, insular, temporal cortices, amygdala, and hippocampus; Module I (43 nodes) in the bilateral occipital, left temporal, and parietal cortices; Module II (36 nodes) in the left sensorimotor, parietal, insular, and temporal regions; and Module III (22 nodes) in the bilateral frontal and cingulate cortices (Fig. 1A). The topological organization of both TSD and NTSD networks was characterized by a significant reduction of subcortical nodal participation in Module V, confining this community to only some regions of the cerebellum and shifting the basal ganglia and thalamus to Module II (Fig. 1B,C). On the other hand, Module III expanded in both patient groups by including the parietal regions in the TSD group and the temporal regions in the NTSD group. Similarly, the expanded Module IV included bilateral sensorimotor, parietal, temporal, and insular regions in both TSD and NTSD patients. Furthermore, while Module remained relatively stable in the NTSD patients compared with healthy participants, the TSD group showed reduction of Module I and expansion of Module II via inclusion of some of the temporal regions of Module I as well as the subcortical and cerebellar regions of Module V.

Both TSD and NTSD groups shared similar network hubs (i.e., nodes with the highest strength and degree values in the network) in the left primary somatosensory (areas 1, 3b), right premotor (area 6 and SMA), and right occipital (areas 17, 18 and hOC3v) cortices (Fig. 2, Table 2). However, the nodal strength of these shared hubs was significantly decreased in NTSD patients compared with healthy participants (25.1 ± 3.6 vs. 31.0 ± 2.9 , corrected $P = 0.02$). Similarly, NTSD patients compared with healthy participants showed network-wide significant decreases in nodal strength (15.3 ± 5.2 vs. 16.9 ± 7.4 , corrected $P = 0.009$) and increases

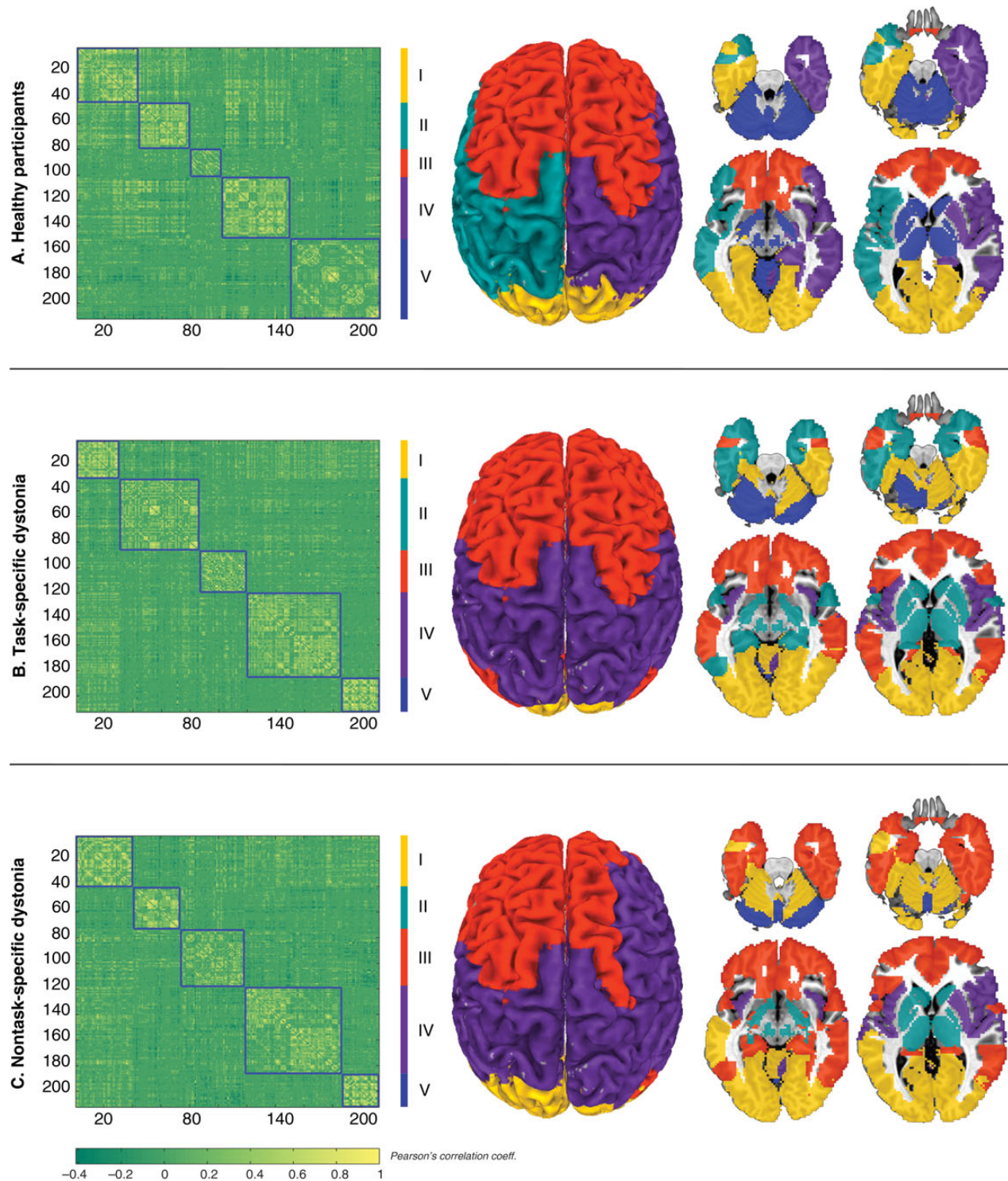


Figure 1. Large-scale community architecture derived from modular decomposition of the group-averaged networks in (A) healthy participants, (B) patients with task-specific dystonia, and (C) patients with nontask-specific dystonia. Left panel shows 212×212 connectivity matrices averaged across each group with the corresponding community partitions. The color bar represents r values based on Pearson's correlation coefficients between each pair of regions. The right panel shows the regional distribution of neural communities on a standard brain in the Talairach–Tournoux space. The 5 network modules are color-coded as follows: yellow = Module I, green = Module II, red = Module III, purple = Module IV, blue = Module V.

in nodal degree (112.2 ± 25.0 vs. 98.5 ± 27.1 , corrected $P = 1.0 \times 10^{-7}$). Such differences, at the level of either shared hubs or the global network, were not found between TSD patients and healthy participants (corrected $P \geq 0.06$).

On the other hand, both TSD and NTSD patients “lost” the left premotor cortex (area 6) as a hub region present in healthy participants (Fig. 2, Table 2). Furthermore, TSD groups formed additional hub regions not present in either healthy participants

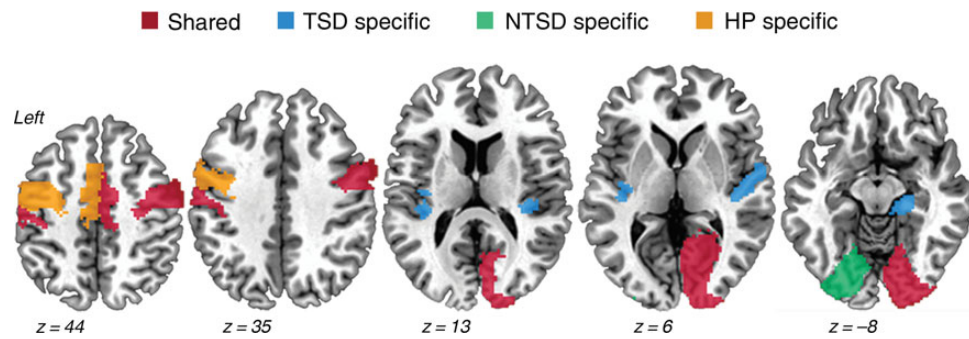


Figure 2. Distribution of shared and distinct hubs. High-strength/high-degree hubs common to healthy participants (HP), patients with task-specific dystonia (TSD), and nontask-specific dystonia (NTSD) are shown in red; hubs unique to TSD patients are shown in blue; hubs unique to NTSD patients are shown in green, and hubs unique to HP are shown in orange. Brain sections are shown as a series of axial slices of a standard brain in the Talairach-Tournoux space.

Table 2 Shared and distinct hubs in the group-averaged networks calculated based on nodal strength and nodal degree

Regions	Nodal strength			Nodal degree		
	HP	TSD	NTSD	HP	TSD	NTSD
Shared hubs between HV, TSD, and NTSD						
L Primary somatosensory cortex (Area 1)	33.4	26.9	24	141	139	138
L Primary somatosensory cortex (Area 3b)	33.6	26.5	22.1	145	129	144
R Occipital cortex (Area 17)	30.3	27.9	27.9	139	127	140
R Occipital cortex (Area 18)	31.8	29	30.6	139	125	148
R Premotor cortex (Area 6)	31.3	25.3	21	156	130	164
R Collateral sulcus (Area hOC3v)	25.8	27.4	25.2	129	129	139
Group mean	31.0	27.2	25.1	141.5	129.8	145.5
Group st. dev.	2.9	1.3	3.6	8.9	4.8	9.8
TSD-specific hubs						
L Insula (Area Ig2)	15.1	26.5	17.6	72	132	92
L Primary auditory cortex (Area TE1.1)	19.0	26.1	17.7	109	141	135
R Hippocampus (Subiculum)	22.2	28.8	19.7	104	137	128
R Primary auditory cortex (Area TE1.0)	16.5	26.4	16.5	69	141	119
R Primary auditory cortex (Area TE1.1)	18.6	24.5	15.8	80	132	128
R Primary auditory cortex (Area TE1.2)	22.7	25.4	16.5	97	124	121
Group mean	19.0	26.3	17.3	88.5	134.5	120.5
Group st. dev.	3.02	1.4	1.4	17.1	6.5	15.1
NTSD-specific hubs						
L Collateral sulcus (Area hOC3v)	19.5	23.5	26.1	93	108	156
L Fusiform gyrus (Area hOC4v)	20.0	23.4	23.7	103	112	138
Group mean	19.8	23.5	24.9	98	110	147
Group st. dev.	0.4	0.1	1.7	7.1	2.8	12.7
HP-specific hubs						
L Premotor cortex (Area 6)	29.4	20.4	17.4	144	113	108
Group mean	29.4	20.4	17.4	144	113	108

Note: The shaded areas highlight the shared and distinct hubs between the groups, with their corresponding group mean and standard deviation values provided in bold. In the NTSD group, the nodal strength of the shared hubs (i.e., the sum of connected edge weights) was significantly decreased compared with healthy participants (corrected $P = 0.02$). No difference in the strength and degree (i.e., the number of connected edges) of shared hubs was observed in the TSD group (corrected $P \geq 0.06$). HP, healthy participants; NTSD, nontask-specific dystonia; TSD task-specific dystonia; L, left; R, right; st. dev., standard deviation.

or NTSD patients, which were located in the left insula (area Ig2), bilateral superior temporal cortex (areas TE 1.0–1.2), and right hippocampus, whereas NTSD patients had additional hubs in the left occipital cortex (areas hOC3v, hOC4v) only (Fig. 2, Table 2).

Independent Component Analysis

Between-group ICA revealed distinct patterns of significant functional connectivity abnormalities of sensorimotor and frontoparietal network components in all patients compared with healthy

participants as well as in TSD compared with NTSD patients. In addition, the comparisons of each form of focal dystonia with healthy participants, although underpowered, yielded similar network abnormalities as reported earlier (Neychev et al. 2011; Zoons et al. 2011) (data not shown).

Generally, the sensorimotor network includes the sensorimotor cortex, supplementary motor area (SMA), and secondary somatosensory cortex, closely corresponding to the brain activation during action execution and perception (Beckmann et al. 2005; Smith et al. 2009) (Fig. 3A–I). Compared with healthy participants, all patients showed extensive bilateral decreases of

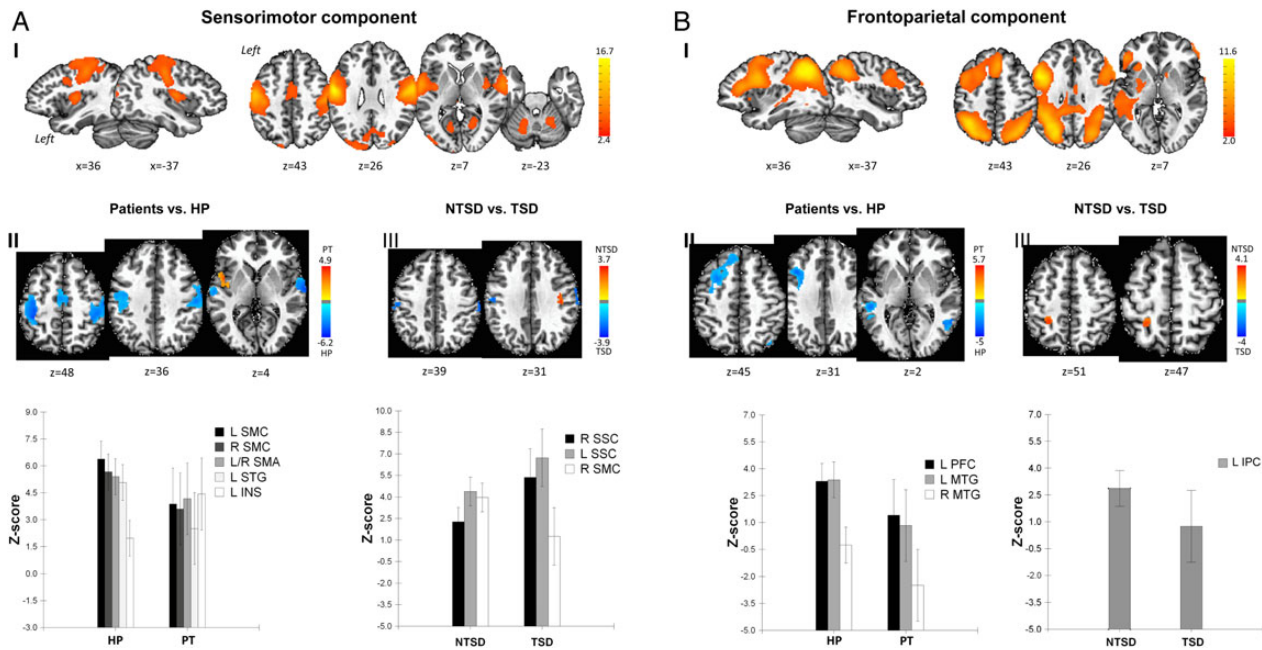


Figure 3. Resting-state functional network alteration assessed using ICA. Panels (A-I) and (B-I) represent the extracted components relevant to dystonia across all patients and healthy participants (A-I for the sensorimotor and B-I for frontoparietal independent components). For each component, voxel-based inferential statistics were used to compare (II) all patients vs. healthy participants, and (III) TSD vs. NTSD groups. Statistical maps are superimposed on axial and sagittal sections of a standard brain in Talairach–Tournoux space. The color bars represent Z-scores for independent components and t scores for group statistical comparisons ($P \leq 0.05$, FWE-corrected). The corresponding bar graphs of the group-averaged resting-state connectivity in the significant clusters are shown in the bottom row of the figure. SMC, sensorimotor cortex; STG, superior temporal gyrus; INS, insula; SSC, somatosensory cortex; PFC, prefrontal cortex; MTG, middle temporal gyrus; IPC, inferior parietal cortex.

functional connectivity in the bilateral primary sensorimotor cortex, SMA, and left superior temporal gyrus (all corrected $P \leq 0.001$) as well as increased connectivity in the left insular cortex (corrected $P = 4.4 \times 10^{-5}$) (Fig. 3A-II, Table 3). Direct comparisons of sensorimotor network between TSD and NTSD groups demonstrated significant differences in functional connectivity in the bilateral primary somatosensory cortex in NTSD patients (all corrected $P \leq 0.005$) and in the right primary sensorimotor cortex in TSD patients (corrected $P = 5.6 \times 10^{-4}$) (Fig. 3A-III, Table 3).

The frontoparietal network is a left lateralized component that comprises extended regions in the parietal, inferior, and middle frontal cortices, strongly corresponding to functional brain activity during cognitive and language processing (Beckmann et al. 2005; Smith et al. 2009) (Fig. 3B-I). Compared with healthy participants, both patient groups exhibited decreased functional connectivity in the left prefrontal cortex and bilateral middle temporal gyrus (all corrected $P \leq 2.9 \times 10^{-4}$) (Fig. 3B-II, Table 3). Direct comparisons between TSD and NTSD patients showed significant differences in functional connectivity in the inferior parietal cortex, extending to the adjacent left primary somatosensory cortex (corrected $P = 0.004$) (Fig. 3B-III, Table 3).

Examination of the mean Z-score values from the significant clusters within the NTSD and TSD groups showed that the observed network differences between these patients were not driven by any single patient subgroup (Kruskal–Wallis nonparametric tests, all $U \geq 11.0$, corrected $P \geq 0.14$).

Relationship Between Different Network Alterations and Their Clinical Correlates

Direct comparisons between significant findings derived from ICA and graph theoretical analysis found overlapping alterations in the primary sensorimotor and premotor cortices, including SMA, and superior temporal gyrus (Fig. 4A). The follow-up

correlation analysis showed a significant positive relationship between abnormal functional connectivity in the SMA and the duration of dystonia (Pearson's correlation coefficient $r = 0.48$, $P = 0.02$), indicating that patients with shorter disease duration had greater impairment of SMA connectivity than patients with longer disease duration (Fig. 4B). Although SMA connectivity was somewhat enhanced in the course of dystonia, it nevertheless did not normalize to the levels observed in healthy participants (Figs 3A-II and 4).

No significant relationships were found between the functional alterations and the severity of dystonia (all $r \leq 0.39$, $P \geq 0.27$).

Discussion

Our study demonstrates widespread re-organization of large-scale functional brain networks in isolated focal dystonia and points to the unified etiopathophysiological mechanism underlying different forms of dystonia due to common network alterations in all patients compared with healthy participants. On the other hand, the presence of distinct alterations of network topology in TSD vs. NTSD provides evidence for additional, pathophysiologically divergent mechanisms potentially contributing to different forms of dystonia.

One of the major common features of abnormal dystonia network topology was the loss of normal hemispheric asymmetry of network community structure in both TSD and NTSD patients compared with healthy participants. This finding appears to reflect disorder-specific network aberrations and is unlikely to be associated with lateralized neurological symptoms as each of the TSD and NTSD groups had 1 patient group with lateralized symptoms (writer's cramp in TSD and cervical dystonia in NTSD) and 1 patient group without lateralized symptoms

Table 3 Brain regions and the corresponding peak locations of the significant clusters showing differences between the groups in the sensorimotor and frontoparietal network components

Brain region	Talairach coordinates (x, y, z)			t-Score
Sensorimotor network				
Patients vs. HP				
Decreases in patients				
R Primary sensorimotor cortex	50	-8	19	6.2
R Supplementary motor areas	6	-14	49	3.8
L Primary sensorimotor cortex	-36	-34	49	5.5
L Superior temporal gyrus	-60	-18	1	3.7
Increases in patients				
L Insula	-44	2	5	4.9
NTSD specific				
R Primary somatosensory cortex	54	-21	39	3.4
L Primary somatosensory cortex	-48	-18	35	3.1
TSD specific				
R Primary sensorimotor cortex	40	-16	41	3.7
Frontoparietal network				
Patients vs. HP				
Decreases in patients				
L Prefrontal cortex	-36	16	31	4.3
L Middle temporal gyrus	-46	-56	5	5.0
R Middle temporal gyrus	50	-58	-1	4.3
TSD specific				
L Inferior parietal cortex	-24	-56	47	3.0

Note: HP, healthy volunteers; NTSD, nontask-specific dystonia; TSD, task-specific dystonia; L, left; R, right.

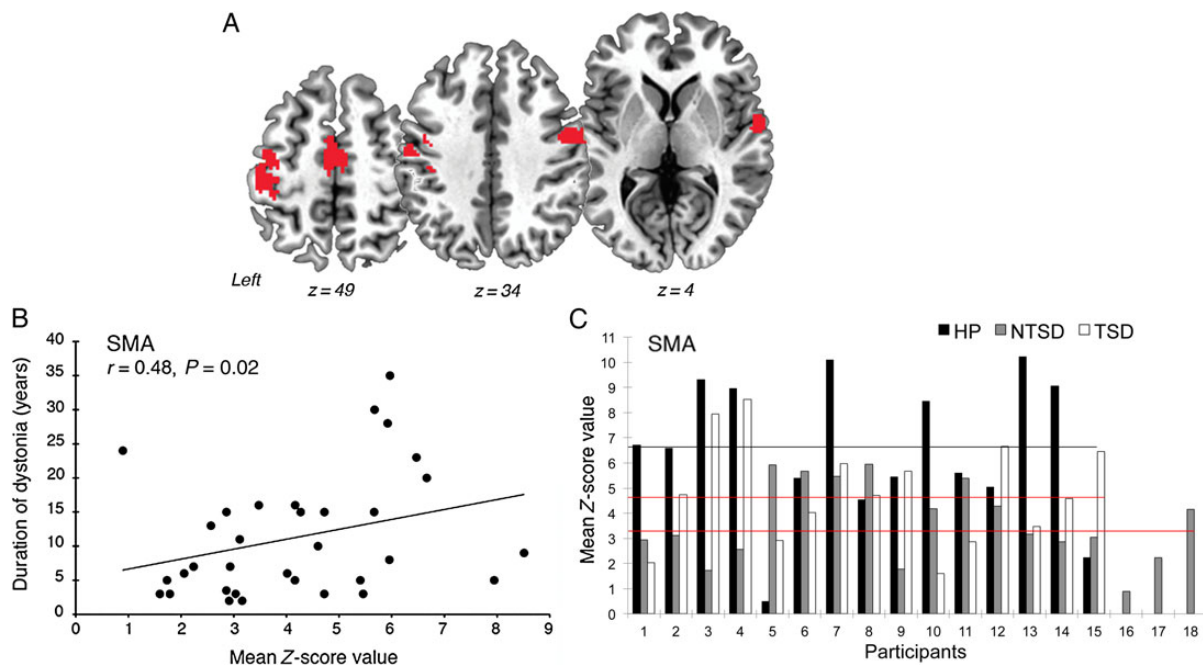


Figure 4. Overlapping alterations in functional connectivity identified with the use of ICA and graph theoretical analysis and their correlates with clinical features of dystonia. (A) The brain regions of overlapping alterations between the significant clusters in the patients vs. healthy participants ICA contrast and the significant hubs in graph analysis (see Figs 2 and 3 for reference) are shown on a series of axial brain slices in the standard Talairach-Tournoux space. For the statistical threshold of the voxels, refer to Figure 3. (B) Scatterplot shows the significant positive correlation between the mean Z-score values in the SMA cluster identified in (A) and dystonia duration in years. (C) Bar graphs show mean Z-score values in the same SMA cluster in all healthy participants (HP), patients with nontask-specific dystonia (NTSD), and patients with task-specific dystonia (TSD). The black line indicates the median of mean Z-score values in the healthy participant group; red lines indicate the median of mean Z-score values in the patient groups.

(spasmodic dysphonia in TSD and blepharospasm in NTSD), which would have counterbalanced the possible bias of symptom lateralization in 1 group vs. another.

Another major shared feature of abnormal network architecture across all forms of dystonia was a breakdown of a single and highly integrated basal ganglia and cerebellar functional

community found in healthy participants into multiple, smaller communities in the patient groups. This network-level finding substantiates well-known regional abnormalities in the basal ganglia and cerebellum, which have been demonstrated in several neuroimaging studies across different forms of focal dystonia (Galardi et al. 1996; Neychev et al. 2008; Mohammadi et al. 2012; Simonyan and Ludlow 2012; Zhou et al. 2013; Hoffland et al. 2014), collectively underscoring the importance of basal ganglia and cerebellar dysfunction in the pathophysiology of this disorder. Our data further suggest that altered functional interactions and loss of integration between the basal ganglia and cerebellar networks may represent a common base for propagation of larger scale network abnormalities, which may jointly contribute to the development of dystonic symptoms. In support of this assumption, we observed a loss of a pivotal region of information transfer (hub) in the left premotor cortex, including the SMA, in both TSD and NTSD patients, despite the overall expansion of their cortical sensorimotor communities. As both basal ganglia and cerebellar networks converge in the motor cortex (Bostan and Strick 2010), our finding may be related to decoupling between these 3 regions and their respective networks. The premotor cortex has been recently a focus of several investigations, which showed abnormal connectivity with the basal ganglia, primary motor, and parietal cortices (Jin et al. 2011; Castrop et al. 2012; Delnooz et al. 2012; Houdayer et al. 2012; Jankowski et al. 2013; Pirio Richardson et al. 2014; Pirio Richardson 2015) as well as improvement of deficits in reciprocal inhibition and mitigation of dystonic symptoms following stimulation of this region (Murse et al. 2000; Huang et al. 2004; Lalli et al. 2012; Veugen et al. 2013; Kimberley et al. 2015). Considering the importance of the premotor cortex, basal ganglia, and cerebellum in different stages of sensorimotor integration, motor learning, and planning, abnormal communication between these regions is likely reflected in altered consolidation of motor programs underlying pathophysiology common to different clinical forms of dystonia. To that end, the SMA is a higher order motor region involved in preparation and initiation of movements and motor learning (Carbonell et al. 2004; Gross et al. 2005), with its activation serving as a neural correlate of inhibition (Ball et al. 1999; Connolly et al. 2000; Mostofsky et al. 2003). The decreased connectivity of the SMA has been previously linked to abnormal inhibition (Mazzini et al. 1994; Naumann et al. 2000; Jin et al. 2011) and abnormal sensorimotor processing in the presence of a sensory trick (Naumann et al. 2000) in patients with focal dystonia. Our finding of a significant relationship between decreased connectivity of SMA and the duration of dystonia points to the impairment of this region from the early years of manifestation of dystonic symptoms.

While the basal ganglia, cerebellar, and premotor cortical connectivity changes are likely to be at the core of pathophysiological alterations of dystonic networks, distinctive functional network abnormalities may be attributed to different forms of isolated focal dystonia. Particularly, we found that dystonias affecting highly learned and skilled movements, such as writing and speaking, showed greater spread of sensorimotor and cognitive/executive network changes than dystonias primarily affecting the performance of involuntary movements, such as eye blinking and neck positioning. These TSD-specific network-level aberrations are in line with earlier findings in another form of TSD, isolated musician's dystonia, which showed that impairment of highly skilled movements involved in playing an instrument was associated with abnormal sensorimotor integration (Rosenkranz et al. 2005), greater alterations of functional activity in the primary sensorimotor cortex (Pujol et al. 2000; Haslinger et al. 2010; Kadota et al. 2010), and

deficient neural synchronization between the sensorimotor cortical regions (Ruiz et al. 2009). Our current study demonstrated that TSD patients have wider spread regional network abnormalities in the primary motor, somatosensory and inferior parietal cortices as opposed to abnormalities in the primary somatosensory cortex alone in NTSD patients. Dystonia has long been known as a motor control disorder (Denny-Brown 1965; Marsden and Quinn 1990), with its primary manifestations including sustained muscle contraction and/or co-contraction of agonist and antagonist muscles (Albanese et al. 2013). However, there has been growing evidence of sensory involvement including the presence of associated sensory symptoms, such as pain (Jankovic et al. 1991; Martino et al. 2005), *geste antagoniste* (Greene and Bressman 1998), abnormal sensory discrimination (Bara-Jimenez et al. 2000; Aglioti et al. 2003; Fiorio et al. 2003, 2007, 2008; Tinazzi et al. 2006; Bradley et al. 2009, 2012), as well as functional and microstructural changes in primary somatosensory cortex (Simonyan and Ludlow 2010; Martino et al. 2011; Suzuki et al. 2011; Delnooz et al. 2012; Prell et al. 2013). Collectively, the findings of our study extend this current knowledge 2-fold by providing experimental evidence for the presence of sensory alterations at the large-scale network level across different forms of dystonia and by suggesting that the pathophysiological basis of task specificity in dystonia may relate to greater abnormalities of sensorimotor integration at the cortical level. Such association of more profound sensorimotor network aberrations in patients with TSD but not NTSD is suggestive of a top-down mechanism in producing dystonic movements during skilled voluntary behaviors.

In this context, the inferior parietal cortex, one of the critical regions for normal sensorimotor processing, was also found to exhibit abnormal functional connectivity and network-wide integration. The parietal cortex, particularly its posterior region, serves as a higher order sensory associative area that, among other functions, integrates somatosensory, visual, and auditory stimuli to create a body scheme prior to the execution of voluntary movements (Andersen 1997; Culham and Valyear 2006; Hickok et al. 2009; Brownsett and Wise 2010; Shum et al. 2011; Sereno and Huang 2014). Decreased connectivity in the parietal cortex may not only impact spatial integration, but also the sense of (self)-agency and attention focusing on task-relevant cognitive, sensory, and motor information (Le et al. 1998; Colby and Goldberg 1999; Farrer and Frith 2002; Gottlieb 2007; Gottlieb et al. 2009). In line with the notion that sensorimotor integration is required for motor planning and execution of voluntary movements (Machado et al. 2010), we demonstrated more complex alterations of the sensorimotor functional connectivity in TSD than in NTSD patients. It is therefore not surprising that the involvement of the inferior parietal cortex may be less critical for the generation of involuntary movements, such as in NTSD patients. In addition, the lesser extent of cortical network changes in NTSD may be attributed to a lesser need for attention as well as sensorimotor and cognitive integration for action creation of internal representation during a more automated task production, such as eye blinking and neck positioning.

However, at the regional level, the NTSD group exhibited significant decreases in nodal strength within the hubs shared by all groups and across the global network as well as network-wide increases in nodal degree. These findings suggest that NTSD patients had either greater disorder-specific regional network abnormalities or, alternatively, the observed nodal changes may have been influenced by the abundant formation of spurious

connections. On the other hand, the large-scale network in TSD patients was characterized by the formation of additional hubs in the insula and superior temporal cortex. The insular cortex has been previously reported to show structural and functional abnormalities in spasmodic dysphonia (Simonyan and Ludlow 2010, 2012), cranio-cervical dystonia (Piccinin et al. 2014), and writer's cramp (Ceballos-Baumann et al. 1997; Lerner et al. 2004). As the insula is involved in several cognitive behaviors including self-awareness of body parts and feeling (Karnath et al. 2005; Craig 2009) and sense of agency (Farrer and Frith 2002), our finding of abnormal hub formation in this region suggests that the creation of internal representation of intended movements may be abnormally enhanced in TSD. In addition, the hub formation in the superior temporal cortex along with decreased functional connectivity of this region within both sensorimotor and frontoparietal networks may have corollary effects on the formation of an abnormal network controlling voluntary attention, which is necessary for execution of any intended movement (Hopfinger et al. 2000).

In conclusion, our data demonstrate that the large-scale neural network is abnormal in isolated focal dystonia and is characterized by greater involvement of cortical alterations in TSD than in NTSD patients. This supports the hypothesis that different forms of dystonia are likely to follow divergent disorder-specific pathophysiological mechanisms.

Funding

This work was supported by Bachmann-Strauss Dystonia and Parkinson Foundation, the National Institutes of Health/National Institute of Neurological Disorders and Stroke (R01NS088160) and National Institute on Deafness and Other Communication Disorders (R01DC011805) grants to K.S., and the National Center for Advancing Translational Sciences (UL1TR000067) grant to Mount Sinai Clinical Research Center. P.T. was supported by a clinical fellowship training program from the Dystonia Medical Research Foundation.

Notes

We thank Amanda Pechman, BA, and Ian Farwell, MSG, for patient recruitment, Lazar Fleysher, PhD, Heather Alexander, BA, Melissa Choy, BA, and Estee Rubien-Thomas, BA, for imaging data acquisition, and Laurie J. Ozelius, PhD, for genetic screening. *Conflict of Interest:* None declared.

References

Aglioti SM, Fiorio M, Forster B, Tinazzi M. 2003. Temporal discrimination of cross-modal and unimodal stimuli in generalized dystonia. *Neurology*. 60:782–785.

Albanese A, Bhatia K, Bressman SB, Delong MR, Fahn S, Fung VS, Hallett M, Jankovic J, Jinnah HA, Klein C, et al. 2013. Phenomenology and classification of dystonia: a consensus update. *Mov Disord*. 28:863–873.

Andersen RA. 1997. Multimodal integration for the representation of space in the posterior parietal cortex. *Philos Trans R Soc London Ser B Biol Sci*. 352:1421–1428.

Asanuma K, Carbon-Correll M, Eidelberg D. 2005. Neuroimaging in human dystonia. *J Med Invest*. 52(Suppl):272–279.

Ashburner J, Friston KJ. 2005. Unified segmentation. *Neuroimage*. 26:839–851.

Ball T, Schreiber A, Feige B, Wagner M, Lucking CH, Kristeva-Feige R. 1999. The role of higher-order motor areas in

voluntary movement as revealed by high-resolution EEG and fMRI. *Neuroimage*. 10:682–694.

Bara-Jimenez W, Shelton P, Hallett M. 2000. Spatial discrimination is abnormal in focal hand dystonia. *Neurology*. 55:1869–1873.

Bassett DS, Bullmore E. 2006. Small-world brain networks. *Neuroscientist*. 12:512–523.

Beckmann CF, DeLuca M, Devlin JT, Smith SM. 2005. Investigations into resting-state connectivity using independent component analysis. *Philos Trans R Soc Lond B Biol Sci*. 360:1001–1013.

Beckmann CF, Smith SM. 2004. Probabilistic independent component analysis for functional magnetic resonance imaging. *IEEE Trans Med Imaging*. 23:137–152.

Berardelli A, Rothwell JC, Day BL, Marsden CD. 1985. Pathophysiology of blepharospasm and oromandibular dystonia. *Brain: J Neurol*. 108(Pt 3):593–608.

Bishop CM. 2006. *Pattern recognition and machine learning*. New York: Springer.

Biswal B, Yetkin FZ, Haughton VM, Hyde JS. 1995. Functional connectivity in the motor cortex of resting human brain using echo-planar MRI. *Magn Reson Med*. 34:537–541.

Blondel VD, Guillaume JL, Lambiotte R, Lefebvre E. 2008. Fast unfolding of communities in large networks. *J Stat Mech-Theory E*. 10:P10008.

Bostan AC, Strick PL. 2010. The cerebellum and basal ganglia are interconnected. *Neuropsychol Rev*. 20:261–270.

Bradley D, Whelan R, Kimmich O, O'Riordan S, Mulrooney N, Brady P, Walsh R, Reilly RB, Hutchinson S, Molloy F, et al. 2012. Temporal discrimination thresholds in adult-onset primary torsion dystonia: an analysis by task type and by dystonia phenotype. *J Neurol*. 259:77–82.

Bradley D, Whelan R, Walsh R, Reilly RB, Hutchinson S, Molloy F, Hutchinson M. 2009. Temporal discrimination threshold: VBM evidence for an endophenotype in adult onset primary torsion dystonia. *Brain: J Neurol*. 132:2327–2335.

Brownsett SL, Wise RJ. 2010. The contribution of the parietal lobes to speaking and writing. *Cereb Cortex*. 20:517–523.

Bullmore E, Sporns O. 2009. Complex brain networks: graph theoretical analysis of structural and functional systems. *Nat Rev Neurosci*. 10:186–198.

Bullmore ET, Bassett DS. 2011. Brain graphs: graphical models of the human brain connectome. *Annu Rev Clin Psychol*. 7:113–140.

Burke RE, Fahn S, Marsden CD, Bressman SB, Moskowitz C, Friedman J. 1985. Validity and reliability of a rating scale for the primary torsion dystonias. *Neurology*. 35:73–77.

Burton K, Farrell K, Li D, Calne DB. 1984. Lesions of the putamen and dystonia: CT and magnetic resonance imaging. *Neurology*. 34:962–965.

Carbon M, Eidelberg D. 2009. Abnormal structure-function relationships in hereditary dystonia. *Neuroscience*. 164:220–229.

Carbon M, Trost M, Ghilardi MF, Eidelberg D. 2004. Abnormal brain networks in primary torsion dystonia. *Adv Neurol*. 94:155–161.

Carbonnell L, Hasbroucq T, Grapperon J, Vidal F. 2004. Response selection and motor areas: a behavioural and electrophysiological study. *Clin Neurophysiol*. 115:2164–2174.

Castrop F, Dresel C, Hennenlotter A, Zimmer C, Haslinger B. 2012. Basal ganglia-premotor dysfunction during movement imagination in writer's cramp. *Mov Disord*. 27:1432–1439.

Ceballos-Baumann AO, Sheean G, Passingham RE, Marsden CD, Brooks DJ. 1997. Botulinum toxin does not reverse the cortical

- dysfunction associated with writer's cramp. A PET study. *Brain: J Neurol.* 120(Pt 4):571–582.
- Colby CL, Goldberg ME. 1999. Space and attention in parietal cortex. *Annu Rev Neurosci.* 22:319–349.
- Connolly JD, Goodale MA, DeSouza JF, Menon RS, Vilis T. 2000. A comparison of frontoparietal fMRI activation during anti-saccades and anti-pointing. *J Neurophysiol.* 84:1645–1655.
- Craig AD. 2009. How do you feel—now? The anterior insula and human awareness. *Nat Rev Neurosci.* 10:59–70.
- Culham JC, Valyear KF. 2006. Human parietal cortex in action. *Curr Opin Neurobiol.* 16:205–212.
- Damoiseaux JS, Greicius MD. 2009. Greater than the sum of its parts: a review of studies combining structural connectivity and resting-state functional connectivity. *Brain Struct Funct.* 213:525–533.
- Delnooz CC, Helmich RC, Toni I, van de Warrenburg BP. 2012. Reduced parietal connectivity with a premotor writing area in writer's cramp. *Mov Disord.* 27:1425–1431.
- Delnooz CC, Pasman JW, Beckmann CF, van de Warrenburg BP. 2013. Task-free functional MRI in cervical dystonia reveals multi-network changes that partially normalize with botulinum toxin. *PLoS ONE.* 8:e62877.
- Denny-Brown D. 1965. The nature of dystonia. *Bull NY Acad Med.* 41:858–869.
- Eickhoff SB, Stephan KE, Mohlberg H, Grefkes C, Fink GR, Amunts K, Zilles K. 2005. A new SPM toolbox for combining probabilistic cytoarchitectonic maps and functional imaging data. *Neuroimage.* 25:1325–1335.
- Eidelberg D, Moeller JR, Antonini A, Kazumata K, Nakamura T, Dhawan V, Spetsieris P, deLeon D, Bressman SB, Fahn S. 1998. Functional brain networks in DYT1 dystonia. *Ann Neurol.* 44:303–312.
- Eidelberg D, Moeller JR, Ishikawa T, Dhawan V, Spetsieris P, Przedborski S, Fahn S. 1995. The metabolic topography of idiopathic torsion dystonia. *Brain.* 118(Pt 6):1473–1484.
- Farrer C, Frith CD. 2002. Experiencing oneself vs another person as being the cause of an action: the neural correlates of the experience of agency. *NeuroImage.* 15:596–603.
- Filippini N, MacIntosh BJ, Hough MG, Goodwin GM, Frisoni GB, Smith SM, Matthews PM, Beckmann CF, Mackay CE. 2009. Distinct patterns of brain activity in young carriers of the APOE-epsilon4 allele. *Proc Natl Acad Sci USA.* 106:7209–7214.
- Fiorio M, Gambarin M, Valente EM, Liberini P, Loi M, Cossu G, Moretto G, Bhatia KP, Defazio G, Aglioti SM, et al. 2007. Defective temporal processing of sensory stimuli in DYT1 mutation carriers: a new endophenotype of dystonia? *Brain.* 130:134–142.
- Fiorio M, Tinazzi M, Bertolasi L, Aglioti SM. 2003. Temporal processing of visuotactile and tactile stimuli in writer's cramp. *Ann Neurol.* 53:630–635.
- Fiorio M, Tinazzi M, Scontrini A, Stanzani C, Gambarin M, Fiaschi A, Moretto G, Fabbrini G, Berardelli A. 2008. Tactile temporal discrimination in patients with blepharospasm. *J Neurol Neurosurg Psychiatry.* 79:796–798.
- Furtinger S, Zinn JC, Simonyan K. 2014. A neural population model incorporating dopaminergic neurotransmission during complex voluntary behaviors. *PLoS Comput Biol.* 10:e1003924.
- Galardi G, Perani D, Grassi F, Bressi S, Amadio S, Antoni M, Comi GC, Canal N, Fazio F. 1996. Basal ganglia and thalamocortical hypermetabolism in patients with spasmodic torticollis. *Acta Neurologica Scandinavica.* 94:172–176.
- Gottlieb J. 2007. From thought to action: the parietal cortex as a bridge between perception, action, and cognition. *Neuron.* 53:9–16.
- Gottlieb J, Balan P, Oristaglio J, Suzuki M. 2009. Parietal control of attentional guidance: the significance of sensory, motivational and motor factors. *Neurobiol Learning Memory.* 91:121–128.
- Greene PE, Bressman S. 1998. Exteroceptive and interoceptive stimuli in dystonia. *Mov Disord.* 13:549–551.
- Gross J, Pollok B, Dirks M, Timmermann L, Butz M, Schnitzler A. 2005. Task-dependent oscillations during unimanual and bimanual movements in the human primary motor cortex and SMA studied with magnetoencephalography. *Neuroimage.* 26:91–98.
- Haslinger B, Altenmuller E, Castrop F, Zimmer C, Dresel C. 2010. Sensorimotor overactivity as a pathophysiologic trait of embouchure dystonia. *Neurology.* 74:1790–1797.
- Hickok G, Okada K, Serences JT. 2009. Area Spt in the human planum temporale supports sensory-motor integration for speech processing. *J Neurophysiol.* 101:2725–2732.
- Hoffland BS, Veugen LC, Janssen MM, Pasman JW, Weerdesteijn V, van de Warrenburg BP. 2014. A gait paradigm reveals different patterns of abnormal cerebellar motor learning in primary focal dystonias. *Cerebellum.* 13:760–766.
- Hopfinger JB, Buonocore MH, Mangun GR. 2000. The neural mechanisms of top-down attentional control. *Nature Neurosci.* 3:284–291.
- Houdayer E, Beck S, Karabanov A, Poston B, Hallett M. 2012. The differential modulation of the ventral premotor-motor interaction during movement initiation is deficient in patients with focal hand dystonia. *Eur J Neurosci.* 35:478–485.
- Huang YZ, Edwards MJ, Bhatia KP, Rothwell JC. 2004. One-Hz repetitive transcranial magnetic stimulation of the premotor cortex alters reciprocal inhibition in DYT1 dystonia. *Mov Disord.* 19:54–59.
- Jankovic J, Leder S, Warner D, Schwartz K. 1991. Cervical dystonia: clinical findings and associated movement disorders. *Neurology.* 41:1088–1091.
- Jankowski J, Paus S, Scheef L, Bewersdorff M, Schild HH, Klockgether T, Boecker H. 2013. Abnormal movement preparation in task-specific focal hand dystonia. *PLoS ONE.* 8:e78234.
- Jin SH, Lin P, Auh S, Hallett M. 2011. Abnormal functional connectivity in focal hand dystonia: mutual information analysis in EEG. *Mov Disord.* 26:1274–1281.
- Jinnah HA, Hess EJ. 2006. A new twist on the anatomy of dystonia: the basal ganglia and the cerebellum? *Neurology.* 67:1740–1741.
- Kadota H, Nakajima Y, Miyazaki M, Sekiguchi H, Kohno Y, Amako M, Arino H, Nemoto K, Sakai N. 2010. An fMRI study of musicians with focal dystonia during tapping tasks. *J Neurol.* 257:1092–1098.
- Karnath HO, Baier B, Nagele T. 2005. Awareness of the functioning of one's own limbs mediated by the insular cortex? *J Neurosci.* 25:7134–7138.
- Kimberley TJ, Borich MR, Schmidt RL, Carey JR, Gillick B. 2015. Focal hand dystonia: individualized intervention with repeated application of repetitive transcranial magnetic stimulation. *Arch Phys Med Rehabilitation.* 96:S122–S128.
- Lalli S, Piacentini S, Franzini A, Panzacchi A, Cerami C, Messina G, Ferre F, Perani D, Albanese A. 2012. Epidural premotor cortical stimulation in primary focal dystonia: clinical and 18F-fluoro deoxyglucose positron emission tomography open study. *Mov Disord.* 27:533–538.

- Le TH, Pardo JV, Hu X. 1998. 4 T-fMRI study of nonspatial shifting of selective attention: cerebellar and parietal contributions. *J Neurophysiol.* 79:1535–1548.
- Leech R, Kamourieh S, Beckmann CF, Sharp DJ. 2011. Fractionating the default mode network: distinct contributions of the ventral and dorsal posterior cingulate cortex to cognitive control. *J Neurosci.* 31:3217–3224.
- Lehericy S, Tijssen MA, Vidailhet M, Kaji R, Meunier S. 2013. The anatomical basis of dystonia: current view using neuroimaging. *Mov Disord.* 28:944–957.
- Lerner A, Shill H, Hanakawa T, Bushara K, Goldfine A, Hallett M. 2004. Regional cerebral blood flow correlates of the severity of writer's cramp symptoms. *NeuroImage.* 21:904–913.
- Machado S, Cunha M, Velasques B, Minc D, Teixeira S, Domingues CA, Silva JG, Bastos VH, Budde H, Cagy M, et al. 2010. Sensorimotor integration: basic concepts, abnormalities related to movement disorders and sensorimotor training-induced cortical reorganization. *Revista de Neurologia.* 51:427–436.
- Marsden CD. 1984. Motor disorders in basal ganglia disease. *Human Neurobiol.* 2:245–250.
- Marsden CD, Quinn NP. 1990. The dystonias. *BMJ.* 300:139–144.
- Martino D, Defazio G, Alessio G, Abbruzzese G, Girlanda P, Tinazzi M, Fabbri G, Marinelli L, Majorana G, Buccafusca M, et al. 2005. Relationship between eye symptoms and blepharospasm: a multicenter case-control study. *Mov Disord.* 20:1564–1570.
- Martino D, Di Giorgio A, D'Ambrosio E, Popolizio T, Macerollo A, Livrea P, Bertolino A, Defazio G. 2011. Cortical gray matter changes in primary blepharospasm: a voxel-based morphometry study. *Mov Disord.* 26:1907–1912.
- Mazzini L, Zaccala M, Balzarini C. 1994. Abnormalities of somatosensory evoked potentials in spasmodic torticollis. *Mov Disord.* 9:426–430.
- Mohammadi B, Kollewe K, Samii A, Beckmann CF, Dengler R, Munte TF. 2012. Changes in resting-state brain networks in writer's cramp. *Hum Brain Mapp.* 33:840–848.
- Mostofsky SH, Schafer JG, Abrams MT, Goldberg MC, Flower AA, Boyce A, Courtney SM, Calhoun VD, Kraut MA, Denckla MB, et al. 2003. fMRI evidence that the neural basis of response inhibition is task-dependent. *Brain Res Cogn Brain Res.* 17:419–430.
- Murase N, Kaji R, Shimazu H, Katayama-Hirota M, Ikeda A, Kohara N, Kimura J, Shibasaki H, Rothwell JC. 2000. Abnormal premovement gating of somatosensory input in writer's cramp. *Brain.* 123(Pt 9):1813–1829.
- Naumann M, Magyar-Lehmann S, Reiners K, Erbguth F, Leenders KL. 2000. Sensory tricks in cervical dystonia: perceptual dysbalance of parietal cortex modulates frontal motor programming. *Ann Neurol.* 47:322–328.
- Neychev VK, Fan X, Mitev VI, Hess EJ, Jinnah HA. 2008. The basal ganglia and cerebellum interact in the expression of dystonic movement. *Brain: J Neurol.* 131:2499–2509.
- Neychev VK, Gross RE, Lehericy S, Hess EJ, Jinnah HA. 2011. The functional neuroanatomy of dystonia. *Neurobiol Dis.* 42:185–201.
- Niethammer M, Carbon M, Argyelan M, Eidelberg D. 2011. Hereditary dystonia as a neurodevelopmental circuit disorder: Evidence from neuroimaging. *Neurobiol Dis.* 42:202–209.
- Piccinin CC, Piovesana LG, Santos MC, Guimaraes RP, De Campos BM, Rezende TJ, Campos LS, Torres FR, Amato-Filho AC, Franca MC Jr, et al. 2014. Diffuse decreased gray matter in patients with idiopathic craniocervical dystonia: a voxel-based morphometry study. *Front Neurol.* 5:283.
- Pirio Richardson S. 2015. Enhanced dorsal premotor-motor inhibition in cervical dystonia. *Clin Neurophysiol.* 126:1387–1391.
- Pirio Richardson S, Beck S, Bliem B, Hallett M. 2014. Abnormal dorsal premotor-motor inhibition in writer's cramp. *Mov Disord.* 29:797–803.
- Prell T, Peschel T, Kohler B, Bokemeyer MH, Dengler R, Gunther A, Grosskreutz J. 2013. Structural brain abnormalities in cervical dystonia. *BMC Neurosci.* 14:123.
- Pujol J, Roset-Llobet J, Rosines-Cubells D, Deus J, Narberhaus B, Valls-Sole J, Capdevila A, Pascual-Leone A. 2000. Brain cortical activation during guitar-induced hand dystonia studied by functional MRI. *NeuroImage.* 12:257–267.
- Quartarone A, Hallett M. 2013. Emerging concepts in the physiological basis of dystonia. *Mov Disord.* 28:958–967.
- Ramdhani RA, Kumar V, Velickovic M, Frucht SJ, Tagliati M, Simonyan K. 2014. What's special about task in dystonia? A voxel-based morphometry and diffusion weighted imaging study. *Mov Disord.* 29:1141–1150.
- Ramdhani RA, Simonyan K. 2013. Primary dystonia: conceptualizing the disorder through a structural brain imaging lens. *Tremor Other Hyperkinet Mov (NY).* 3:pil: tre-03-152-3638-4.
- Rosenkranz K, Williamon A, Butler K, Cordivari C, Lees AJ, Rothwell JC. 2005. Pathophysiological differences between musician's dystonia and writer's cramp. *Brain.* 128:918–931.
- Rubinov M, Sporns O. 2010. Complex network measures of brain connectivity: uses and interpretations. *Neuroimage.* 52:1059–1069.
- Ruiz MH, Senghaas P, Grossbach M, Jabusch HC, Bangert M, Hummel F, Gerloff C, Altenmüller E. 2009. Defective inhibition and inter-regional phase synchronization in pianists with musician's dystonia: an EEG study. *Hum Brain Mapp.* 30:2689–2700.
- Sereno MI, Huang RS. 2014. Multisensory maps in parietal cortex. *Curr Opin Neurobiol.* 24:39–46.
- Shu N, Liu Y, Li K, Duan Y, Wang J, Yu C, Dong H, Ye J, He Y. 2011. Diffusion tensor tractography reveals disrupted topological efficiency in white matter structural networks in multiple sclerosis. *Cereb Cortex.* 21:2565–2577.
- Shum M, Shiller DM, Baum SR, Gracco VL. 2011. Sensorimotor integration for speech motor learning involves the inferior parietal cortex. *Eur J Neurosci.* 34:1817–1822.
- Simonyan K, Ludlow CL. 2010. Abnormal activation of the primary somatosensory cortex in spasmodic dysphonia: an fMRI study. *Cereb Cortex.* 20:2749–2759.
- Simonyan K, Ludlow CL. 2012. Abnormal structure-function relationship in spasmodic dysphonia. *Cereb Cortex.* 22:417–425.
- Smith SM, Fox PT, Miller KL, Glahn DC, Fox PM, Mackay CE, Filippini N, Watkins KE, Toro R, Laird AR, et al. 2009. Correspondence of the brain's functional architecture during activation and rest. *Proc Natl Acad Sci USA.* 106:13040–13045.
- Sun Y, Danila B, Josic K, Bassler KE. 2009. Improved community structure detection using a modified fine-tuning strategy. *Epl-Europhys Lett.* 86(2), 28004:1–6.
- Suzuki Y, Kiyosawa M, Wakakura M, Mochizuki M, Ishii K. 2011. Gray matter density increase in the primary sensorimotor cortex in long-term essential blepharospasm. *NeuroImage.* 56:1–7.
- Tinazzi M, Fiorio M, Stanzani C, Moretto G, Smania N, Fiaschi A, Bhatia KP, Rothwell JC. 2006. Temporal discrimination of two passive movements in writer's cramp. *Mov Disord.* 21:1131–1135.

- Veugen LC, Hoffland BS, Stegeman DF, van de Warrenburg BP. 2013. Inhibition of the dorsal premotor cortex does not repair surround inhibition in writer's cramp patients. *Exp Brain Res*. 225:85–92.
- Yang J, Luo C, Song W, Chen Q, Chen K, Chen X, Huang X, Gong Q, Shang H. 2013. Altered regional spontaneous neuronal activity in blepharospasm: a resting state fMRI study. *J Neurol*. 260:2754–2760.
- Zhou B, Wang J, Huang Y, Yang Y, Gong Q, Zhou D. 2013. A resting state functional magnetic resonance imaging study of patients with benign essential blepharospasm. *J Neuroophthalmol*. 33:235–240.
- Zoons E, Booij J, Nederveen AJ, Dijk JM, Tijssen MA. 2011. Structural, functional and molecular imaging of the brain in primary focal dystonia—a review. *Neuroimage*. 56:1011–1020.